Bending-rigidity-driven transition and crumpling-point scaling of lattice vesicles

E. Orlandini
Department of Physics, Theoretical Physics, University of Oxford, Oxford OX1 3NP, England

A. L. Stella
INFM-Dipartimento di Fisica e Sezione INFN, Università di Padova, I-35131 Padova, Italy

T. L. Einstein
Department of Physics, University of Maryland, College Park, Maryland 20742-4111

M. C. Tesi
Mathematical Institute, University of Oxford, Oxford OX1 3LB, England

I. Beichl
Computing and Applied Mathematics Laboratory, National Institute of Standards and Technology, Gaithersburg, Maryland 20899

F. Sullivan
Center for Computing Sciences, 17100 Science Drive, Bowie, Maryland 20715-4300

The crumpling transition of three-dimensional (3D) lattice vesicles subject to a bending fugacity $\rho = \exp(-\kappa/k_B T)$ is investigated by Monte Carlo methods in a grand canonical framework. By also exploiting conjectures suggested by previous rigorous results, a critical regime with scaling behavior in the universality class of branched polymers is found to exist for $\rho > \rho_c$. For $\rho < \rho_c$ the vesicles undergo a first-order transition that has remarkable similarities to the line of droplet singularities of inflated 2D vesicles. At the crumpling point ($\rho = \rho_c$), which has a tricritical character, the average radius and the canonical partition function of vesicles with n plaquettes scale as n^{ν_c} and $n^{-\theta_c}$, respectively, with $\nu_c = 0.4825 \pm 0.0015$ and $\theta_c = 1.78 \pm 0.03$. These exponents indicate a new class, distinct from that of branched polymers, for scaling at the crumpling point. [S1063-651X(96)10705-4]

I. INTRODUCTION

Models of membranes and vesicles have been investigated extensively in recent years. Such models are presumed to describe large-scale fluctuation properties of molecular aggregates such as those forming the interfaces of microemulsions or the lipid bilayers of biological membranes [1,2]. These are highly flexible, topologically two-dimensional structures with fixed area, the conformations of which are primarily controlled by bending rigidity. In the case of closed shapes (e.g., spherical vesicles), a pressure difference Δp between the interior and the exterior may also influence the shape and its fluctuations.

In many instances, such as the above examples, molecules are able to diffuse within the aggregate and do not take fixed relative positions forming a lattice. Such fluid membranes are often described by tethered surfaces [1], with (annealed) tethers that can be suitably cut and rejoined [3]. These models should be distinguished from solid tethered surfaces, where (quenched) tethers form a fixed network [4]. Another way to describe fluid vesicles (i.e., those with zero shear elasticity) is to use lattice surfaces made of elementary plaquettes [5–9]. Here we adopt this description and deal with a model of self-avoiding plaquette surfaces (SAS) of spherical topology on a cubic lattice.

Many important issues concerning lattice SAS and, more generally, surface models have been addressed succesfully in recent years, especially with the aid of efficient Monte Carlo algorithms. Today, e.g., there is no doubt that a spherical SAS with no bending rigidity and no pressure difference behaves like a branched polymer (BP) asymptotically, as the number of plaquettes approaches infinity [8,10–13]. This property also persists after one removes the topological constraint of requiring zero genus and so allows the SAS to form an unrestricted number of handles [14]. The effects of an osmotic pressure (Δp) are also rather well understood in the absence of bending rigidity. Under deflation ($\Delta p < 0$) the vesicles maintain the BP critical behavior of the flaccid, $\Delta p = 0$, regime [15,16]. However, any inflation, no matter how small, causes maximal-volume configurations to become dominant. The transition between flaccid ($\Delta p = 0$) and inflated ($\Delta p > 0$) regimes is first order and has been interpreted [17] in terms of droplet singularities [18,19]. Another process that is by now well understood in many respects is vesicle adsorption by an attracting plane [20].

A central issue in the statistics of membrane and vesicle models is the effect of bending rigidity [21], even in the absence of pressure increments [3,22–24]. By introducing local bending rigidity in a closed-surface model, one expects that spherical (cubic in the lattice case) configurations will dominate at very high rigidity. For low rigidity, on the other hand, the highly ramified, crumpled BP behavior should be

recovered for fluid vesicles, while a different, but still crumpled regime could possibly prevail for solid tethered surfaces. Whether the rigid and crumpled regimes are separated by a crumpling transition occurring at intermediate rigidity and, if so, the nature of this transition are important, unresolved, and controversial questions in the statistical mechanics of random surfaces: While many theoretical approaches do predict such transitions [25–27], their nature remains rather obscure, and numerical work casts doubt on their very existence [3]. For example, in the case of both ''solid'' and fluid tethered surfaces, the existence of the transition seems to be ruled out when the self-avoidance constraint is enforced [3,22,28,29]. The situation appears different for self-avoiding lattice surfaces. Monte Carlo methods in both the grand canonical [24] and canonical [23] ensembles provide evidence of such a transition. There are also indications, albeit not definitive, that the transition is continuous [23]. In any case, the scaling properties at this possibly continuous transition have not been determined to date; the state at the crumpling threshold has not been characterized precisely. *The essence of this work is to confirm definitively the crumpling transition in lattice SAS and to provide a systematic and accurate characterization of the associated scaling properties.*

Our results are based on a Monte Carlo algorithm in the grand canonical ensemble, introduced earlier for lattice SAS [12]. This ensemble allows easier study of both entropic and metric scaling properties, which are key ingredients in the characterization of scaling at the crumpling point. Moreover, in this ensemble we can exploit easily some previous rigorous results for SAS [30], which aid our search dramatically. Thus, we combine the high efficiency and precision of our Monte Carlo algorithm with analytic information to obtain the most convenient and natural path to our objectives.

The study of the crumpling transition in a lattice context offers a unique opportunity to explore nontrivial relations between apparently distinct and unconnected aspects of vesicle physics. One such relation is indeed established here between the phase diagram of pressurized, rigid vesicles in two dimensions (2D) [17] and that of our flaccid and rigid vesicles in 3D. This relationship proves essential in locating the crumpling point and in characterizing its critical behavior, and might offer a hint towards understanding the very existence of a crumpling transition for lattice surfaces.

This paper is organized as follows: In Sec. II the model is introduced, and the grand canonical formalism is set up. In Sec. II we also give a summary and partial reinterpretation of previously obtained rigorous limits and bounds related to the model. In Sec. III we present the results of a first global analysis of the phase diagram of the model. We determine the nature of the different critical and first-order lines and estimate exponents and other asymptotic properties. In Sec. IV, making use of results of the previous analysis, we carry out a systematic study of entropic and conformational scaling properties at the crumpling transition. Section V contains further discussion and some concluding remarks.

II. MODEL, EXACT RESULTS, AND MONTE CARLO APPROACH

In order to describe a 3D vesicle, one can consider a closed self-avoiding surface constructed by gluing together elementary plaquettes (unit squares of Z^3) in such a way that neither overlaps nor intersections occur. Each lattice plaquette can enter only once to form the SAS, and each lattice edge of the vesicle can be shared by only two plaquettes. Moreover, we shall confine our attention to vesicles that are homeomorphic to the sphere: our vesicles are connected and have no handles. The generating function of vesicles with curvature interaction can be written as

$$G_q(K,\rho) = \sum_{n,l_p} v(n,l_p) n^q K^n \rho^{l_p} = \sum_n n^q K^n Z_n(\rho), \quad (1)$$

where $v(n,l_p)$ is the number of vesicles with n plaquettes and l_p edges joining two mutually perpendicular plaquettes. In v and G_q a normalization per lattice site in the thermodynamic limit is implicit. The parameter K is a plaquette fugacity (perhaps more precisely, an absolute activity) associated with the grand canonical ensemble in equilibrium with a plaquette reservoir. The factor n^q in the summand is introduced to allow an analysis of entropic exponents ($q > 3/2$ is needed, and we choose $q = 3$ as a rule), and generally to enhance the sampling of surfaces with large area [12]. The parameter ρ is the Boltzmann factor related to the stiffness energy κ by

$$\rho = \exp\left(-\frac{\kappa}{k_B T}\right). \quad (2)$$

Clearly the smaller ρ, the stronger the tendency of the vesicle to assume flat configurations. Z_n is a canonical partition function at fixed n. Typically in polymer statistics one expects various canonical and grand canonical quantities to obey asymptotic laws characterized by entropic or thermal exponents, if the asymptotics themselves are consistent with second-order, continuous critical behavior. This situation occurs often. However, there are exceptions, as we will find below, in which first-order, discontinuous behavior occurs.

The canonical partition function in a critical regime should behave like

$$Z_n(\rho) = \sum_{l_p} v(n,l_p)\rho^{l_p} \underset{n\to\infty}{\sim} n^{-\theta}[K_c(\rho)]^{-n}, \quad (3)$$

where θ is the entropic exponent. For $\rho = 1$, Z_n is the number of distinct vesicle configurations with n plaquettes. Evaluation of θ by directly fitting Monte Carlo data with Eq. (3) is not expected to be very successful. A much better strategy, which we follow below, consists of extracting θ from the behavior of the grand canonical average area of the vesicle plotted as a function of K [12]. An example of a grand canonical average yielding the thermal exponent ν is

$$R^2(K,\rho) = \frac{\sum_n Z_n(\rho) n^q K^n R_n^2(\rho)}{G_q(K,\rho)} \underset{K\to K_c(\rho)^-}{\sim} [K_c(\rho) - K]^{-2\nu}, \quad (4)$$

where $R_n^2(\rho) = Z_n(\rho)^{-1} \sum_{l_p} v(n,l_p) R^2(n,l_p)\rho^{l_p}$ is the canonical mean-square radius of gyration, with respect to the center of mass, of surfaces with area n and arbitrary l_p. Equation (4) is also equivalent to the canonical law

$$R_n^2(\rho) \underset{n \to \infty}{\sim} n^{2\nu}. \qquad (5)$$

In a recent paper, Baumgärtner studied the crumpling transition in a canonical context, i.e., starting from a canonical partition such as $Z_n(\rho)$ [23]. However, he did not consider entropic exponents, and his analysis of metric properties did not provide clear conclusions, especially about the nature of the crumpling transition [31].

The main goal of our study, which extends earlier, preliminary efforts [24], is to determine how quantities such as K_c or ν and θ depend on ρ. Of course, we are mostly interested in the case $\rho < 1$, where the tendency to crumple and ramify spontaneously is opposed by the bending rigidity. For ν and θ we expect some degree of universality. It is possible for these exponents to remain constant over whole intervals of ρ values. Such intervals would correspond to universality domains of critical behavior.

For the model described by Eqs. (2.1)–(2), Whittington recently studied the limit of the canonical free energy as a function of ρ and, on the basis of rigorous inequalities and concatenation arguments, established upper and lower bounds for the critical curve $K_c(\rho)$ [30]. In particular he found that, for all real values of ρ, the free-energy limit

$$F(\rho) \equiv \lim_{n \to \infty} \frac{1}{n} \ln Z_n(\rho) \qquad (6)$$

converges to a finite value:

$$F(\rho) = -\ln K_c(\rho) < \infty, \qquad (7)$$

which is a convex function of $\ln\rho$. The bounds on $K_c(\rho)$ are given by

$$K_c(1) \leq K_c(\rho) \leq 1, \quad \rho \leq 1, \qquad (8)$$

$$K_c(1)\rho^{-2} \leq K_c(\rho) \leq \min[K_c(1),\rho^{-2}], \quad \rho \geq 1, \qquad (9)$$

where $K_c(1)$ is the critical fugacity of vesicles with no rigidity [12].

Unfortunately, the rigorous techniques used by Whittington are not sufficiently powerful to establish whether, and for which value of ρ, a crumpling transition, i.e. a drastic change in the exponents, might occur. Neither can they estimate the exponents at that transition. However, as we shall discuss below, the above inequalities can be used to formulate plausible conjectures that help us greatly in the numerical investigations.

The inequality (8), which holds particular significance for us, can be justified easily: Suppose we restrict the vesicle configurations contributing to G_q to those having the shape of a (flat, rigid) wafer of unit thickness. When projected onto some arbitrarily chosen principal plane, such wafer configurations can be described as self-avoiding rings (on a square net). The statistics of such configurations are in fact the same as for 2D vesicles with disk topology. Each plaquette enclosed by the ring has weight K^2, while each boundary edge has weight $x = K\rho^2$. An additional bending fugacity ρ has to be associated with each pair of consecutive links on the perimeter that meet at right angles. In terms of generating functions we have

$$G_q(K,\rho) \geq \sum_{\text{2D vesicles}} (K^2)^A x^p \rho^{n_p}, \qquad (10)$$

where A and p are the area and the perimeter of the 2D vesicle, respectively, while n_p is the number of consecutive-edge pairs at right angles along the ring. So we are clearly left with a model of 2D rigid vesicles, with fugacities controlling perimeter and area. Since the slab configurations form a subset of the total, the generating function for the 2D vesicles cannot exceed G_q. On the other hand, we know that the 2D vesicle generating function is infinite as soon as $K^2 > 1$ (corresponding to $\Delta p > 0$), as a consequence of droplet singularities [18,19]. In this case with rigidity, the radius-of-convergence reasoning (based on area versus perimeter terms) in Eq. (10) follows straightforwardly from arguments developed in Ref. [17] for pressurized vesicles (see also Ref. 30). We conclude that G_q must already be infinite for $K > 1$, i.e., $K_c \leq 1$. Since there is no well-defined phase above $K_c(\rho)$, we use the expression ''singularity curve'' rather than ''phase boundary.''

In order to gain more insight into the crumpling transition for lattice vesicles, we turn to the numerical approach of Monte Carlo simulations. Our Monte Carlo strategy samples configurations of vesicles from a Markov chain having as its limiting distribution the one considered in Eq. (1). The main innovation of our algorithm is an oct-tree data structure, which allows satisfactory control of the statistics, even when the model is very close to criticality. Details of the sampling method, the error estimates, and the data analysis have been described thoroughly in Ref. [12], and so are not discussed here.

III. NUMERICAL RESULTS AND PHASE DIAGRAM

In this section we report data on the ρ dependence of several grand canonical quantities. Based on our estimates of the singularity curve, $K_c = K_c(\rho)$, and on the rigorous bounds mentioned in the previous section, we conjecture that the singularities in the high-rigidity regime ($\rho < \rho_c$) have a first-order, dropletlike nature [17]. The crumpling-transition point ($\rho = \rho_c$) is thus interpreted as a sort of tricritical point located at the end of the droplet line. As a matter of fact, it turns out that the previously discussed bound $K_c(\rho) \leq 1$ plays a key role in the determination of the phase diagram because numerical evidence clearly locates the droplet line precisely at $K_c = 1$. The physics of 2D pressurized vesicles, from which this bound originates, is somehow connected to the rigidity-driven transition in our system. The line of first-order (essential) singularities we find here does seem to be interpretable in terms of the similar line existing for vesicles in 2D at zero pressure difference. In spite of the strong numerical evidence supporting the scenario described above, we cannot entirely rule out the possibility that $K_c(\rho) < 1$, for all ρ [32]. This alternative picture would still be consistent with the presence of a transition corresponding to a change of convexity in $K_c(\rho)$.

In our numerical investigation we proceeded as follows: For each chosen value of ρ we performed long Monte Carlo (MC) runs at several values of K. For each value of the plaquette fugacity we estimated grand canonical averages of the form

TABLE I. Estimates of some grand canonical averages coming from Monte Carlo sampling at $\rho=0.7$ for various values of K.

K	$\langle S \rangle_q$	$\langle V \rangle_q$	$\langle R^2 \rangle_q$
0.850	41.49 ± 0.1	12.03 ± 0.1	3.008 ± 0.04
0.860	53.07 ± 0.2	16.08 ± 0.1	3.855 ± 0.04
0.870	69.48 ± 0.3	21.99 ± 0.2	5.038 ± 0.05
0.875	85.58 ± 0.5	28.02 ± 0.2	6.184 ± 0.06
0.880	103.19 ± 0.7	37.17 ± 0.3	8.006 ± 0.07
0.882	118.32 ± 0.8	41.49 ± 0.4	8.771 ± 0.08
0.884	133.65 ± 0.9	46.15 ± 0.4	9.668 ± 0.08
0.888	160.60 ± 1.5	69.17 ± 0.8	14.14 ± 0.20
0.890	204.74 ± 2.7	77.77 ± 1.0	15.33 ± 0.23
0.892	260.03 ± 3.7	113.36 ± 1.8	22.57 ± 0.35
0.894	340.53 ± 5.0	135.22 ± 2.5	25.96 ± 0.38

$$\langle A \rangle_q = G_q(\rho,K)^{-1} \sum_{n,l_p} v(n,l_p) A(n,l_p) n^q K^n \rho^{l_p}, \quad (11)$$

where $A(n,l_p)$ indicates the average of the generic quantity A at fixed n and l_p.

For illustrative purposes quantities estimated for fixed $\rho=0.7$ are reported in Table I. There V indicates the volume enclosed by the vesicle. Proceeding as in Ref. [12], we estimated the exponent ν by fitting to Eq. (4). In the case reported in Table I, we obtained $\nu=0.501\pm0.004$ (two standard deviations). $K_c(\rho)$ and θ are best determined from plots of $\langle S \rangle_q^{-1}$ versus K, noting that

$$\langle S \rangle_q \sim \frac{K_c(\rho)(q+1-\theta)}{K_c(\rho)-K} \quad \text{for } K \to K_c^-. \quad (12)$$

Again, the case $\rho=0.7$ (see Table I) gives $K_c(0.7)=0.901\pm0.009$ and $\theta=1.51\pm0.03$. We also estimated the asymptotic behavior of the surface-to-volume ratio $\langle S \rangle_q / \langle V \rangle_q$ and the ratio of the average number of edge pairs joining two plaquettes perpendicular to each other (the quantity conjugate to the bending energy) to the surface area, $\langle l_p \rangle_q / \langle S \rangle_q$. We find that these ratios approach constant values (~ 2.597 and ~ 1.111, respectively) as $K \to K_c^-$.

All the steps described above were repeated for various values of ρ ranging from 0.64 to 2.0. Since we are interested in the crumpling transition, the most interesting region for us
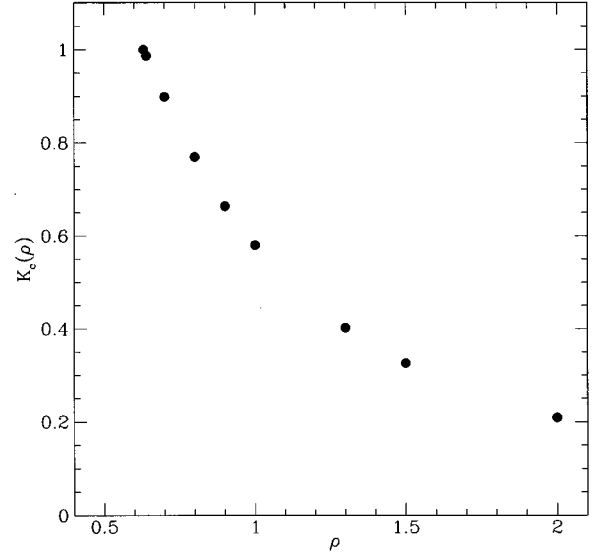

FIG. 1. Numerical estimate of the critical curve K_c for various values of the bending fugacity ρ.

is the one with $\rho<1$. The estimates of the relevant extrapolated quantities are reported in Table II.

From the data in Table II, we can draw some preliminary conclusions. As ρ decreases, $K_c(\rho)$ increases and approaches the value 1 quite rapidly, the maximum value allowed by the rigorous bound (8). The limiting value, $K_c=1$, is first attained for $\rho=\rho_c\approx0.635$. The numerical estimates of $K_c(\rho)$ suggest that $K_c(\rho)$ is a convex function of ρ for $\rho_c \lesssim \rho \lesssim 2.0$ (see Fig. 1). It is thus natural to conclude that K_c should reach the value 1 at some finite value ρ_c. Once this is assumed, the rigorous bound (8) together with monotonic variation [30] imply that, for all $\rho<\rho_c$, $K_c=1$.

The estimated values of ν and θ reported in Table II suggest that over the entire range considered ($0.64<\rho\leq2.0$), the vesicle critical behavior belongs to the universality class of BP in $d=3$. In fact, the determinations of the entropic exponent θ and the metric exponent ν agree, to within error bars, with the values $\frac{3}{2}$ and $\frac{1}{2}$, respectively, expected for 3D BP [33]. The only exceptions are the determinations at $\rho=0.64$, where we can see, at least for θ, strong deviations from the BP value; we will consider this problem below.

Further evidence that ramified tubular configurations

TABLE II. Numerical estimate of the critical curve $K_c(\rho)$ and of various universal quantities as a function of the bending fugacity ρ.

ρ	$K_c(\rho)$	θ	ν	$\langle S \rangle_q / \langle V \rangle_q$	$\langle l_p \rangle_q / \langle S \rangle_q$
2.0	0.209 ± 0.010	1.51 ± 0.08	0.518 ± 0.020	3.64 ± 0.010	1.592 ± 0.001
1.5	0.326 ± 0.008	1.51 ± 0.08	0.512 ± 0.010	3.53 ± 0.011	1.479 ± 0.001
1.3	0.402 ± 0.007	1.49 ± 0.07	0.514 ± 0.008	3.46 ± 0.014	1.433 ± 0.001
1.0	0.580 ± 0.005	1.50 ± 0.05	0.506 ± 0.005	3.27 ± 0.014	1.339 ± 0.001
0.9	0.664 ± 0.006	1.51 ± 0.06	0.507 ± 0.005	3.11 ± 0.014	1.293 ± 0.002
0.8	0.770 ± 0.007	1.51 ± 0.05	0.505 ± 0.005	2.90 ± 0.015	1.225 ± 0.002
0.7	0.899 ± 0.009	1.51 ± 0.03	0.501 ± 0.004	2.60 ± 0.015	1.111 ± 0.004
0.64	0.987 ± 0.010	1.70 ± 0.03	0.488 ± 0.003	2.14 ± 0.013	0.978 ± 0.002

dominate the statistics of vesicles in this range of ρ is given by the asymptotic behavior of the surface-to-volume ratio. The limit of this ratio being a constant means that the volume enclosed by the vesicle grows to infinity like the surface area of the vesicle. Another result consistent with BP behavior is that asymptotically the average number of edges joining two mutually perpendicular plaquettes $\langle l_p \rangle_q$ varies linearly with the average surface area $\langle S \rangle_q$.

At fixed $\rho < \rho_c$, as we try to approach the line $K = 1$ from below, we see no trace of critical behavior (such as the divergence of $\langle S \rangle_q$, for example). On the other hand, if we choose K slightly above one, we find a system out of equilibrium in which the plaquette number and the size of the sampled vesicle configurations grow without bound as a run proceeds. These configurations are like maximal area disks, or thin ''wafers.'' Their thickness is close to unity for $\rho \lesssim \rho_c$ and increases gradually with decreasing ρ.

This situation is similar to that occurring in the 2D vesicle model with pressure difference Δp when one crosses the line of essential singularities separating the region of the finite ramified deflated vesicle $\Delta p < 0$ from the nonequilibrium region of the inflated square-shaped vesicles ($\Delta p > 0$) (see Ref. [17]). In our rederivation of the bound $K_c(\rho) \leq 1$ at the end of the previous section, we established that this bound follows from the fact that the generating function for 2D vesicles with area fugacity K^2, perimeter fugacity $x = \rho^2 K$, and rigidity ρ is always a lower bound of G_q. For $\rho < \rho_c$ and $K \lesssim 1$, the statistics of our 3D vesicles appear to be dominated by finite configurations similar to the waferlike ones providing the lower bound of G_q.

The analogy to the droplet transition of the 2D vesicle model with osmotic pressure and rigidity can be made even stronger: for $K > 1$ we observe that the surface area S grows indefinitely with time while the number of edges l_p grows as the square root of S. This behavior translates into the perimeter growing like the square root of area for inflated 2D vesicles. Further evidence of the waferlike configurations is provided by the observation that the volume of the vesicles grows proportionally to the area.

From these considerations we conjecture that the model of 3D vesicles with rigidity displays the same type of phase diagram as the 2D vesicle model with pressure. In particular, we claim that the semi-infinite line $K = 1$ and $\rho < \rho_c$ constitutes a locus of droplet (first-order) singularities for the problem (see Fig. 2). Thus, the point $(\rho_c, 1)$, which governs the crumpling transition of the model should correspond to a tricritical point, i.e., a point where a first-order line joins a second-order one.

There is support for the intriguing possibility of an even deeper connection between the droplet-singularities line of rigid 3D vesicles found here and that of pressurized, rigid 2D vesicles: Recalling that $K_c(\rho) = 1$ so that $x_c = \rho_c^2$, we find $\rho_c^2 \simeq 0.40$, quite close to the best estimate of the critical boundary step fugacity for the 2D self-avoiding rings in the flaccid regime ($x_c = 0.379\,0526 \pm 0.000\,0005$ [35]). We already observed that along the droplet line, $\rho \lesssim \rho_c$, $K = 1$, our 3D vesicles appear to behave similarly to minimal-thickness wafers, with boundary perimeter weight $x = \rho^2$ and rigidity fugacity ρ. The critical instability of the 3D vesicles occurs very close to that of the strictly 2D model of self-avoiding
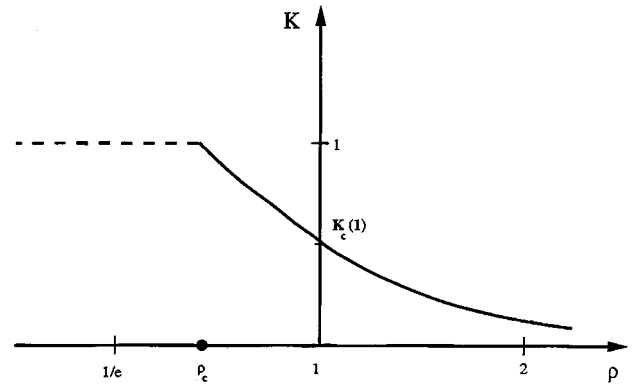

FIG. 2. Schematic plot of the K vs ρ phase diagram. Along the dashed horizontal segment $\rho \leq \rho_c$, $K = 1$, there is a locus of droplet singularities.

rings with step fugacity x and vanishing stiffness energy. Indeed, for a 2D ring without rigidity, the critical step fugacity should be $x_c(\rho = 1) = 0.3790, \ldots$; for a ring subject to some rigidity $\rho \approx 0.63$, we can only say that the critical step fugacity $x_c(\rho)$ should not be lower $[x_c(\rho) \geq x_c(1)]$. While we suspect the shift of this step fugacity from the value $x_c(1)$ to be small, we cannot provide a quantitative estimate. The remarkable closeness of ρ_c^2 to the critical step fugacity of 2D rings seems to suggest a deeper link between critical scaling of 3D vesicles at the crumpling point and 2D multicritical pressurized vesicles. However, as we discuss in the next sections, this approximate coincidence does not imply that the instability is identical in the two cases. The 3D character of our vesicles at the crumpling threshold is unambiguously manifested and cannot be simply traced back to some model, such as 2D self-avoiding rings, embedded in a lower-dimensional space.

IV. MORE PRECISE CHARACTERIZATION OF THE CRUMPLING TRANSITION

From the discussion in the previous section, it seems natural to try to locate more precisely the tricritical point by fixing the plaquette fugacity K at 1 and performing runs at several different $\rho < \rho_c$. Our results are reported in Table III.

A plot of $\langle S \rangle_q^{-1}$ versus ρ^{-1} gives linear behavior with slope $a = 0.259 \pm 0.002$ and intercept $b = -0.411 \pm 0.002$. From the ratio $-a/b$, we can estimate

$$\rho_c = 0.63 \pm 0.01, \tag{13}$$

TABLE III. Numerical estimate of the mean area as a function of the bending fugacity ρ for $\rho < \rho_c$.

ρ	$\langle S \rangle_q$
0.600	47.33 ± 0.76
0.610	72.18 ± 2.34
0.620	138.11 ± 16.83
0.623	194.84 ± 22.26
0.624	238.18 ± 47.90
0.625	264.26 ± 45.03
0.627	397.08 ± 48.48

TABLE IV. Numerical estimate of different grand canonical averages at $\rho = \rho_c$ and for several values of the surface fugacity K approaching the suggested critical value $K_c(\rho_c) = 1$.

K	$\langle S \rangle_q$	$\langle V \rangle_q$	$\langle R^2 \rangle_q$	$\langle l_p \rangle_q$	$\mathcal{A}_{|S|}$	$\mathcal{D}_{|S|}$	$\mathcal{S}_{|S|}$
0.960	52.9 ± 0.2	17.3 ± 0.1	3.86 ± 0.02	60.1 ± 0.2	1.010 ± 0.006	0.295 ± 0.006	0.041 ± 0.003
0.970	70.3 ± 0.3	24.3 ± 0.1	5.12 ± 0.02	77.2 ± 0.3	0.970 ± 0.006	0.293 ± 0.007	0.041 ± 0.003
0.980	105.9 ± 0.7	39.6 ± 0.3	7.67 ± 0.05	112.0 ± 0.6	0.930 ± 0.006	0.292 ± 0.011	0.041 ± 0.005
0.984	132.6 ± 0.8	51.8 ± 0.4	9.52 ± 0.06	127.8 ± 0.8	0.920 ± 0.006	0.285 ± 0.035	0.035 ± 0.006
0.990	217.4 ± 3.2	92.44 ± 1.7	15.43 ± 0.23	217.6 ± 2.9	0.890 ± 0.009	0.284 ± 0.025	0.034 ± 0.008
0.992	263.2 ± 4.0	115.9 ± 2.5	18.42 ± 0.26	260.2 ± 3.5	0.880 ± 0.008	0.277 ± 0.023	0.029 ± 0.006
0.993	304.2 ± 4.9	136.9 ± 2.8	21.26 ± 0.35	298.0 ± 4.4	0.870 ± 0.010	0.292 ± 0.026	0.040 ± 0.009
0.994	340.2 ± 4.9	155.1 ± 2.8	23.69 ± 0.36	331.6 ± 4.4	0.860 ± 0.010	0.292 ± 0.026	0.041 ± 0.009
0.995	394.8 ± 5.4	183.3 ± 3.0	27.37 ± 0.40	382.6 ± 4.9	0.860 ± 0.010	0.291 ± 0.026	0.040 ± 0.011
0.997	556.8 ± 7.2	269.8 ± 4.4	38.12 ± 0.50	531.5 ± 6.4	0.860 ± 0.010	0.290 ± 0.028	0.040 ± 0.013

consistent with the value 0.635 of the previous section obtained from runs at constant ρ.

In order to study the crumpling transition more closely, we set ρ to the last estimated value of $\rho_c = 0.63$ and performed several long runs for different values of $K < K(\rho_c) = 1$ to get precise estimates of the exponents. In addition to the grand canonical averages of the area, volume, squared radius of gyration, and number of edges with perpendicular plaquettes, we computed three different, supposedly universal, quantities related to the eigenvalues $(\lambda_1 < \lambda_2 < \lambda_3)$ of the inertial tensor of the vesicles. More precisely if $(r_k^{(1)}, r_k^{(2)}, r_k^{(3)})$ are the components of the position $\vec{r}_k$ locating the center of the kth plaquette, we define the inertial tensor of a configuration with n plaquettes as

$$\mathcal{G}_{\alpha\beta} = \frac{1}{2(n+1)^2} \sum_{k=0}^{n} \sum_{m=0}^{n} (r_k^{(\alpha)} - r_m^{(\alpha)})(r_k^{(\beta)} - r_m^{(\beta)}). \quad (14)$$

The asymmetry measures $\mathcal{A}$, $\mathcal{D}$, and $\mathcal{S}$ are then defined [36] as

$$\mathcal{A} \equiv \lim_{|S| \to \infty} \mathcal{A}_{|S|}, \quad \text{with} \quad \mathcal{A}_{|S|} = \langle \lambda_1 / \lambda_3 \rangle_q, \quad (15)$$

$$\mathcal{D} \equiv \frac{3}{2} \lim_{|S| \to \infty} \mathcal{D}_{|S|}, \quad \text{with} \quad \mathcal{D}_{|S|} = \frac{\langle \text{Tr}\{[\mathcal{G} - \mathcal{I}\text{Tr}(\mathcal{G})/3]^2\}\rangle_q}{\langle [\text{Tr}(\mathcal{G})]^2 \rangle_q}, \quad (16)$$

$$\mathcal{S} \equiv \frac{9}{2} \lim_{|S| \to \infty} \mathcal{S}_{|S|}, \quad \text{with} \quad \mathcal{S}_{|S|} = \frac{\langle \text{Tr}\{[\mathcal{G} - \mathcal{I}\text{Tr}(\mathcal{G})/3]^3\}\rangle_q}{\langle [\text{Tr}(\mathcal{G})]^3 \rangle_q}, \quad (17)$$

where $\mathcal{I}$ is the unit tensor. Our estimates of all seven averages for 10 values of K are displayed in Table IV. Also in these computations we determined $K_c(\rho_c)$ and θ by plotting $\langle S \rangle_q^{-1}$ versus K^{-1} [see Eq. (12)]. The result $K_c(\rho_c) = 1.0004 \pm 0.0100$ is in very good agreement with the value 1 conjectured in the previous section, while for the entropic exponent we estimate

$$\theta_c = 1.78 \pm 0.03, \quad (18)$$

where the error bars are obtained by taking into account the estimates of θ and ν at $\rho = 0.62$ and 0.64. Even if we take

three standard deviations for the error bars, the estimate of the entropic exponent at the crumpling transition is definitely larger than the corresponding value $\theta = \frac{3}{2}$ of 3D branched polymers.

A determination of the exponent ν by fitting Eq. (4) gives

$$2\nu_c = 0.972 \pm 0.001. \quad (19)$$

Alternatively, ν can be estimated from data collected over realizations of vesicles for several runs at different values of K. Let $N_K(n)$ be the number of vesicles of size n realized in a run with fugacity K. Let $\langle R^2 \rangle_{n,K}$ be the canonical mean square radius of gyration over this sample. Then over all the runs (at various values of K), we compute

$$\langle R^2 \rangle_n = \frac{\Sigma_K N_K(n) \langle R^2 \rangle_{n,K}}{\Sigma_K N_K(n)}, \quad (20)$$

which is a weighted average over the averages from the individual runs: the weights are proportional to the sample sizes. The data are displayed in Fig. 3. To compute ν we
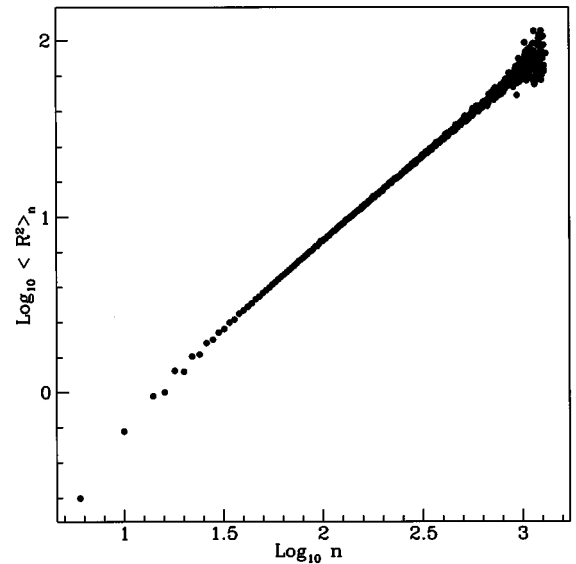

FIG. 3. Log-log plot (with common logarithms) of the canonical mean-squared radius of gyration at $\rho = \rho_c$.

assume the scaling form given by Eq. (5), ignoring higher-order corrections. A linear least-squares fit gives

$$2\nu_c = 0.9650 \pm 0.0030, \tag{21}$$

where the error bars are estimated as in Eq. (18). Evidently the two methods give comparable estimates of ν_c at the crumpling transition; these estimates are slightly, but decidedly, lower than the expected value of ν for BP in $d=3$ [33]. If $\nu < 1/2$ then at crumpling the vesicle configurations cannot remain strictly waferlike: we know that, for such disks, $\nu = 1/2$ should apply [34].

For the two ratios $\langle S \rangle_q / \langle V \rangle_q$ and $\langle l_p \rangle_q / \langle S \rangle_q$, we obtained 1.94 ± 0.02 and 0.930 ± 0.002, respectively. In particular, the nonzero value of the latter asymptotic ratio is further evidence that we are not dealing with waferlike vesicles at this crumpling threshold. Furthermore, for waferlike vesicles a surface-to-volume ratio exactly equal to 2 should be expected. Our value is close, but three standard deviations smaller.

From Table IV it is also possible to extrapolate the universal quantities $\mathcal{A}$, $\mathcal{D}$, and $\mathcal{S}$ as $K \to K_c(\rho_c)$. The results are

$$\mathcal{A} = 0.86 \pm 0.02, \tag{22}$$

$$\mathcal{D} = 0.29 \pm 0.03, \tag{23}$$

$$\mathcal{S} = 0.040 \pm 0.015. \tag{24}$$

Comparing these estimates with ϵ expansion ($\mathcal{D} = 0.326$ and $\mathcal{S} = 0.164$, to order ϵ^1) or series estimates ($\mathcal{D} = 0.390 \pm 0.003$ and $\mathcal{S} = 0.27 \pm 0.01$) for 3D BP [37], we see that these universal quantities are also different at the crumpling point from in the crumpled regime.

V. SUMMARY AND DISCUSSION

From a systematic MC study of a plaquette vesicle model subject to bending rigidity and self-avoidance, we have obtained strong evidence of the existence of three distinct singular regimes as a function of the stiffness fugacity ρ. For moderate rigidity ($\rho > \rho_c$), the vesicle maintains the asymptotic scaling properties of a BP, as already well established for the zero-rigidity case. Here singular behavior exhibits continuous, second-order character with BP exponents as K approaches $K_c(\rho)$. This critical fugacity is a decreasing function of ρ in this range and appears consistent with rigorous bounds [30]. In the high-rigidity region ($\rho < \rho_c$), we have strong numerical evidence that the singularity line occurs at the upper-bound value for the fugacity, i.e., $K_c = 1$. This result is again consistent with the rigorous bounds of Ref. [30]. Along this line there is clear evidence that vesicles undergo a first-order divergence very similar to that occurring for 2D pressurized vesicles. For $K \leq K_c(\rho) = 1$, the vesicles remain finite, and there is no indication of critical scaling. However, once $K > 1$, the configurations grow without bound, as indicated by the lack of a finite equilibration time. Thus, the transition can be explicitly described in terms of droplet singularities [19]. In the $K > 1$ regime, the growing vesicles are predominantly thin disks, with minimal perimeter (i.e., l_p) for given area.

These waferlike configurations and the physical interpre-

tation of the upper bound on K_c suggest a close relation between the rigidity-driven droplet line here and the inflation threshold of 2D vesicles. It is certainly intriguing that we found ρ_c^2 close to $x_c(1) = 0.37, \ldots$. We know that $\rho_c^2 \leq x_c(\rho_c)$, and $x_c(1) \leq x_c(\rho_c)$. Presumably $x_c(\rho_c) - x_c(1)$ is also very small.

The above results and the clear features of the phase diagram established in our analysis allowed us to locate the transition very precisely and to examine carefully the peculiar critical regime at ρ_c. This crumpling point evidently exhibits a tricritical nature and is characterized by a θ exponent that differs from the BP one. An unusual universality class is then realized at the crumpling transition. While ν_c differs less distinctly from the BP value, the fact that it appears to be slightly lower than 1/2 is probably not an artifact of the analysis. In his attempt to assess the critical exponents of the transition for the same model, Baumgärtner also reported values less than 1/2 for ν_c [23].

An important aspect of our study was the assessment of the extent to which crumpling point scaling deviates from that to be expected from a simple 2D picture of slab configurations. Our analysis showed that crumpling point scaling is associated with a genuinely 3D critical instability.

The notion that crumpling point scaling differs from that of multicritical 2D vesicles is further supported by the following argument: If the critical rigid vesicle at $\rho = \rho_c$ behaved as an essentially 2D object, the entropic exponent should be that appropriate to express the number of configurations of planar self-avoiding rings in terms of their enclosed area. This exponent is well known [38], and its conjectured exact value would imply $\theta_c = 1$, which is very far from our estimate.

In view of the aforementioned failure of various attempts to establish the existence of a crumpling transition in models of tethered surfaces, we believe our results are certainly remarkable. We still lack a complete understanding of what peculiar features of latticized surfaces could allow them to display a crumpling point that is not present in the continuum [39]. However, our results suggest that a crucial ingredient in rigid-lattice vesicles is the possibility of establishing a direct link with 2D vesicles under pressure, which are well known to possess a droplet line with a tricritical point [17]. A similar relation in the context of tethered surface models does not seem obvious to us. To establish it would certainly imply substantial modifications of the existing models. Thus, we suspect that a major role in determining the very existence of a crumpling transition in our model is played by the evident relation found here between pressurized and rigid vesicles in the lattice context.

[1] Contributions in *Statistical Mechanics of Membranes and Surfaces*, edited by D.R. Nelson, T. Piran, and S. Weinberg (World Scientific, Singapore, 1989).

[2] R. Lipowsky, Nature **349**, 475 (1991).

[3] G. Gompper and D.M. Kroll, Phys. Rev. E **51**, 514 (1995).

[4] Y. Kantor, M. Kardar, and D.R. Nelson, Phys. Rev. Lett. **57**, 791 (1986).

[5] A. Maritan and A.L. Stella, Phys. Rev. Lett. **53**, 123 (1984).

[6] B. Durhuus, J. Fröhlich, and T. Jonsson, Nucl. Phys. **B225** **[FS9]**, 185 (1983).

[7] B. Durhuus, J. Fröhlich, and T. Jonsson, Nucl. Phys. **B240** **[FS12]**, 453 (1984).

[8] U. Glaus, J. Stat. Phys. **50**, 1141 (1988).

[9] J. Fröhlich, in *Applications of Field Theory to Statistical Mechanics*, edited by L. Garrido, Lectures Notes in Physics Vol. 216 (Springer, Berlin, 1985), p. 31.

[10] U. Glaus, Phys. Rev. Lett. **56**, 1986 (1986).

[11] U. Glaus and T.L. Einstein, J. Phys. A **20**, L105 (1987).

[12] J. O'Connell, F. Sullivan, D. Libes, E. Orlandini, M.C. Tesi, A.L. Stella, and T.L. Einstein, J. Phys. A **24**, 4619 (1991).

[13] A. Baumgärtner and A. Romero, Physica A **187**, 243 (1992).

[14] A.L. Stella, E. Orlandini, I. Beichl, F. Sullivan, M.C. Tesi, and T.L. Einstein, Phys. Rev. Lett. **69**, 3650 (1992).

[15] E. Orlandini and M.C. Tesi, Physica A **185**, 160 (1992).

[16] A. Baumgärtner, Physica A **190**, 62 (1992).

[17] M.E. Fisher, A.J. Guttmann, and S.G. Whittington, J. Phys. A **24**, 3095 (1991).

[18] A.F. Andreev, Zh. Éksp. Teor. Fiz. **45**, 2064 (1963) [Sov. Phys. JETP **18**, 1415 (1964)].

[19] M.E. Fisher, Physics **3**, 1415 (1967); in *Proceedings of the Gibbs Symposium: Yale University, 1989*, edited by D.G. Caldi and G.D. Mostow (American Mathematical Society, Providence, 1990), p. 39.

[20] E. Orlandini, A.L. Stella, M.C. Tesi, and F. Sullivan, Phys. Rev. E **48**, R4203 (1993).

[21] S. Leibler, R.R.P. Singh, and M.E. Fisher, Phys. Rev. Lett. **59**, 1989 (1987).

[22] D.M. Kroll and G. Gompper, Science **255**, 968 (1992).

[23] A. Baumgärtner, Physica A **192**, 550 (1993).

[24] A.L. Stella, Turkish J. Phys. **18**, 244 (1994).

[25] D.R. Nelson and L. Peliti, J. Phys. (Paris) **48**, 1085 (1987).

[26] M. Kardar and D.R. Nelson, Phys. Rev. A **38**, 966 (1988).

[27] E. Guitter, F. David, S. Leibler, and L. Peliti, J. Phys. (Paris) **50**, 1787 (1987).

[28] Y. Kantor and D.R. Nelson, Phys. Rev. A **36**, 4020 (1987).

[29] F.F. Abraham, W. Rudge, and M. Plischke, Phys. Rev. Lett. **62**, 1757 (1989). The results of this paper cast serious doubts on the existence of a crumpling transition claimed in Ref. [28].

[30] S.G. Whittington, J. Math. Chem. **14**, 103 (1993).

[31] Notice that the partition function in Ref. [23] has a different choice of normalization of the rigidity term in the Boltzmann factor. In our case the Boltzmann factor is $\exp[-l_p(\kappa/k_BT)]$, while in his case it is $\exp[-(l_p/2n)(\kappa/k_BT)]$. His choice was unconventional but inconsequential in his ensemble.

[32] E.J. Janse van Rensburg (private communication).

[33] G. Parisi and N. Sourlas, Phys. Rev. Lett. **46**, 871 (1981).

[34] J. Banavar, A. Maritan, and A. Stella, Phys. Rev. A **43**, 5752 (1991).

[35] A.J. Guttman and I.G. Enting, J. Phys. A **21**, L165 (1988).

[36] V. Privman, P.C. Hohenberg, and A. Aharony, in *Phase Transitions and Critical Phenomena*, edited by C. Domb and J.L. Lebowitz (Academic, New York, 1993), Vol. 14.

[37] J. P. Straley and M. J. Stephen, J. Phys. A **20**, 6501 (1987).

[38] I.G. Enting and A.J. Guttman, J. Stat. Phys. **58**, 475 (1990).

[39] The recollection that roughening only occurs in lattice models does not provide the answer. The crumpling transition is distinct: e.g., it leads to an increase in the Hausdorff dimension, in contrast to roughening. See Sec. 3 of Ref. [9].